

# Process Modeling of CO<sub>2</sub> Injection into Natural Gas Reservoirs for Carbon Sequestration and Enhanced Gas Recovery

C. M. Oldenburg,\* K. Pruess, and S. M. Benson

Earth Sciences Division, Lawrence Berkeley National Laboratory, Berkeley, California 94720

Received October 25, 2000. Revised Manuscript Received January 15, 2001

Injection of CO<sub>2</sub> into depleted natural gas reservoirs offers the potential to sequester carbon while simultaneously enhancing CH<sub>4</sub> recovery. Enhanced CH<sub>4</sub> recovery can partially offset the costs of CO<sub>2</sub> injection. With the goal of analyzing the feasibility of carbon sequestration with enhanced gas recovery (CSEGR), we are investigating the physical processes associated with injecting CO<sub>2</sub> into natural gas reservoirs. The properties of natural gas reservoirs and CO<sub>2</sub> and CH<sub>4</sub> appear to favor CSEGR. To simulate the processes of CSEGR, a module for the TOUGH2 reservoir simulator that includes water, brine, CO<sub>2</sub>, tracer, and CH<sub>4</sub> in nonisothermal conditions has been developed. Simulations based on the Rio Vista Gas Field in the Central Valley of California are used to test the feasibility of CSEGR using CO<sub>2</sub> separated from flue gas generated by the 680 MW Antioch gas-fired power plant. Model results show that CO<sub>2</sub> injection allows additional CH<sub>4</sub> to be produced during and after CO<sub>2</sub> injection.

## Introduction

Depleted natural gas reservoirs are potentially important targets for carbon sequestration by direct carbon dioxide (CO<sub>2</sub>) injection. The accumulation and entrapment of a light gas such as methane (CH<sub>4</sub>) testifies to the integrity of natural gas reservoirs for containing gas for long periods of time. By virtue of their proven record of gas production, depleted natural gas reservoirs have demonstrated histories of both (i) available volume, and (ii) integrity against gas escape. The IEA (International Energy Agency) has estimated that as much as 140 GtC could be sequestered in depleted natural gas reservoirs worldwide<sup>1</sup> and 10 to 25 GtC in the United States alone.<sup>2</sup> These aspects of natural gas reservoirs for carbon sequestration are widely recognized.

Less well recognized is the potential utility of CO<sub>2</sub> injection into natural gas reservoirs for the purpose of enhancing CH<sub>4</sub> production by simple repressurization of the reservoir. The pressure support provided by the CO<sub>2</sub> is similar to the proven cushion gas concept used in the gas storage industry wherein expansion of cushion gases upon natural gas withdrawal aids in production from the storage reservoir.<sup>3,4</sup> The concept of enhancing CH<sub>4</sub> production is important because it can partially offset the costs of CO<sub>2</sub> sequestration. This concept was first described by van der Burgt et al.<sup>5</sup> and Blok et al.<sup>6</sup> who used reservoir simulation to evaluate

how quickly the injected CO<sub>2</sub> would mix with the produced natural gas. On the basis of the simulations they concluded that enhanced production was possible for some period before the extent of mixing was too great. Nevertheless, little attention has been given to this option for sequestration, primarily due to concerns about degrading the quality of the produced gas. As for the enhanced gas recovery part of the process, existing economics are not favorable for enhancing gas recovery by CO<sub>2</sub> injection, a situation that could change if carbon tax programs are implemented in the future.

The purpose of this paper is to present results of our research into the physical processes involved in CSEGR. Numerical simulations of CO<sub>2</sub> injection and enhanced gas recovery were carried out on a model system based on the Rio Vista Gas Field in California's Central Valley. The proposed source of CO<sub>2</sub> in this study is flue gas from the 680 MW power plant at Antioch, California, 20 km from Rio Vista. To carry out the simulations, we have developed capabilities for the TOUGH2 reservoir simulator<sup>7</sup> for modeling gas reservoirs. Through simulations of the injection process, we show that repressurization of the CH<sub>4</sub> is possible and significant quantities of CH<sub>4</sub> that would otherwise be left in the reservoir can be produced during and after CO<sub>2</sub> injection.

## Process Description

CSEGR involves the injection of CO<sub>2</sub> into depleted gas reservoirs with simultaneous or subsequent production

\* Author to whom correspondence should be addressed. Voice: (510) 486-7419. Fax: (510) 486-5686. E-mail: cmoldenburg@lbl.gov.

(1) IEA, *Carbon Dioxide Utilization*, IEA Greenhouse Gas R&D Programme: 1997; Table 6.

(2) Riechle et al. *Carbon sequestration research and development*, U.S. Department of Energy: 2000; DOE/SC/FE-1.

(3) Carrière, J. F.; Fasanino, G.; Tek, M. R. *Society of Petroleum Engineers* **1985**, *SPE-14202*, 9–12.

(4) Laille, J.-P.; Molinard, J.-E.; Wents, A. *Soc. Pet. Eng. J.* **1988**, *SPE-17740*, 343–352.

(5) van der Burgt, M. J.; Cantle, J.; Boutkan, V. K. *Energy Convers. Manage.* **1992**, *33* (5–8), 603–610.

(6) Blok, K.; Williams, R. H.; Katofsky, R. E.; Hendriks, C. A. *Energy* **1997**, *22* (2–3), 161–168.

(7) Pruess, K.; Oldenburg, C.; Moridis, G. *TOUGH2 user's guide, version 2.0*; Lawrence Berkeley National Laboratory Report: 1999; LBNL-43134 (<http://esd.lbl.gov/TOUGH2>).

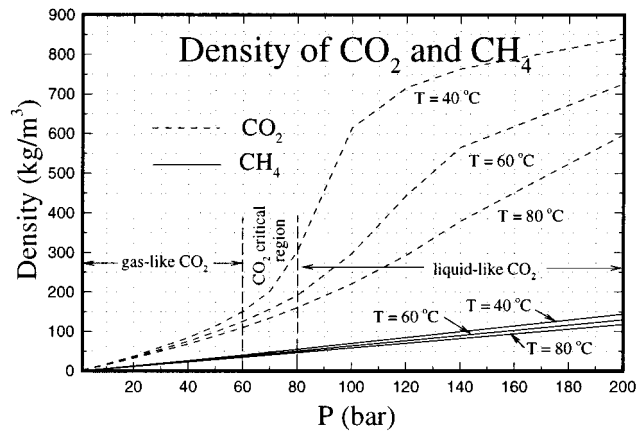


**Figure 1.** Density of CO<sub>2</sub> and CH<sub>4</sub> at  $T = 40, 60,$  and  $80\text{ }^{\circ}\text{C}$  as a function of pressure based on data from Vargaftik.<sup>8</sup> Note the gaslike and liquidlike regions for CO<sub>2</sub>.

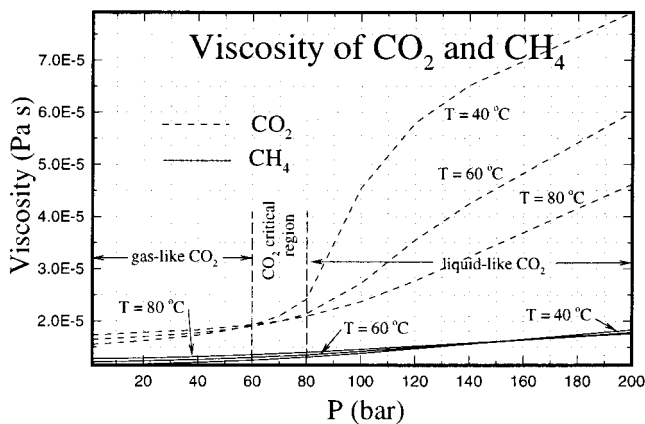


**Figure 2.** Viscosity of CO<sub>2</sub> and CH<sub>4</sub> at  $T = 40, 60,$  and  $80\text{ }^{\circ}\text{C}$  as a function of pressure based on data from Vargaftik.<sup>8</sup>

**Table 1. Properties of CO<sub>2</sub> and CH<sub>4</sub><sup>a</sup>**

property	CO <sub>2</sub>	CH <sub>4</sub>
molecular weight	44 g/mol	16 g/mol
critical point	31 °C, 74 bar	-83 °C, 46 bar
diffusivity (at 273 K, 1 bar)	$1.42 \times 10^{-5} \text{ m}^2/\text{s}$ (in air)	$1.53 \times 10^{-5} \text{ m}^2/\text{s}$ (in CO <sub>2</sub> )

<sup>a</sup> Ref 8.

of repressurized CH<sub>4</sub>. The processes of miscible mixing of the gases by advection, dispersion, and molecular diffusion, which will tend to mix the gaseous components and deteriorate the quality of the natural gas, are dependent on the properties of natural gas reservoirs and of the gases. Pressures in depleted natural gas reservoirs are approximately 20–50 bar, with temperatures 27–120 °C. The large volume and large areal extent of gas reservoirs decrease the potential for mixing by dispersion over practical time scales. In Figures 1 and 2, and Table 1,<sup>8</sup> we present properties of CO<sub>2</sub> and CH<sub>4</sub> relevant to CSEGR. Note that CO<sub>2</sub> is denser and more viscous than CH<sub>4</sub> at all relevant conditions for gas reservoirs and that CO<sub>2</sub> will generally be subcritical but may be supercritical in deep depleted reservoirs. The large density of CO<sub>2</sub> relative to CH<sub>4</sub> means that CO<sub>2</sub> will tend to migrate downward relative to CH<sub>4</sub>. The larger viscosity of CO<sub>2</sub> ensures that displacement of CH<sub>4</sub> by CO<sub>2</sub> will be a favorable mobility ratio displacement,

(8) Vargaftik, N. B. *Tables on the thermophysical properties of liquids and gases*, 2nd ed.; John Wiley & Sons: New York, 1975.

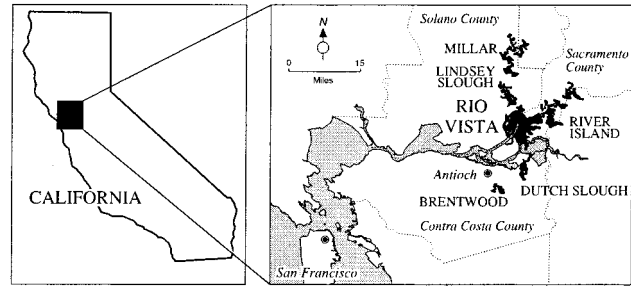


**Figure 3.** Rio Vista Gas Field area map showing gas fields in black.

with less tendency for the gases to finger and intermix than in displacements such as water floods in oil reservoirs. Furthermore, pressure diffusivity is typically three–five orders of magnitude larger than molecular diffusivity, making repressurization occur much faster than mixing by molecular diffusion. In summary, the properties of gas reservoirs and CO<sub>2</sub> and CH<sub>4</sub> appear to favor the feasibility of CSEGR by potentially limiting the amount of mixing between the gases.

### Mathematical Model

To model gas reservoir processes, we have developed a module called EOS7C<sup>9</sup> for simulating gas and water flow in natural gas reservoirs within the TOUGH2 framework.<sup>7</sup> TOUGH2 is an integral finite difference multiphase and multicomponent subsurface flow and transport simulator widely used in the fields of geothermal energy and nuclear waste isolation studies. The EOS7C module handles five components (water, brine, noncondensable gas, tracer, and methane) along with heat. The noncondensable gas can be selected by the user to be CO<sub>2</sub>, N<sub>2</sub>, or air. EOS7C is an extension of the EOS7R<sup>10</sup> and EWASG<sup>11</sup> modules. The EOS7C module is currently restricted to the high-temperature “gaslike” conditions when CO<sub>2</sub> is present as opposed to the high-pressure “liquidlike” conditions (see Figure 1). This restriction to gaslike conditions for CO<sub>2</sub> arises from the ideal gas approximation used in EOS7C. For pressures less than 50 bar, this approximation results in underprediction of pure CO<sub>2</sub> gas density by less than 5%. When only CH<sub>4</sub> and water are present, the module is applicable over a wide range of pressures from 1 bar to well over 126 bar. Simple mixing relations are used for calculating density, viscosity, and phase-partitioning properties of gas mixtures composed of water vapor, CO<sub>2</sub>, and CH<sub>4</sub>. While the accuracy of these mixing relations and ideal gas approximation remain to be evaluated against more sophisticated equations of state, the present model is considered an adequate model of gas mixture properties for simulating the main reservoir processes involved in CSEGR in depleted reservoirs. Advection of gas and liquid phases is governed by a multiphase extension of Darcy’s law. Molecular diffusion in the gas and liquid phases is currently modeled using

(9) Oldenburg, C. M.; Pruess, K. *EOS7C: Gas reservoir simulation for TOUGH2*; Lawrence Berkeley National Laboratory Report: 2001, in preparation.

(10) Oldenburg, C. M.; Pruess, K. *EOS7R: Radionuclide transport for TOUGH2*; Lawrence Berkeley National Laboratory Report: 1995; LBL-34868.

(11) Battistelli, A.; Calore, C.; Pruess, K. *Geothermics* **1997**, 26 (4), 437–464.

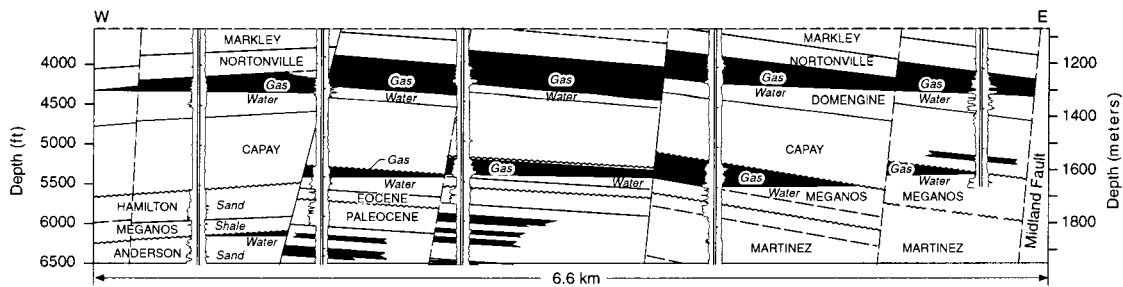


Figure 4. East-west cross section of the Rio Vista Gas Field modified from Burroughs.<sup>15</sup>

a Fickian approach. The main gas species partition between the gas and liquid phases according to their temperature- and pressure-dependent solubilities,<sup>12–14</sup> while the gas tracer volatilization is controlled by a Henry's coefficient input by the user. The selection of N<sub>2</sub> or air in place of CO<sub>2</sub> will allow the module to be used for simulating gas storage processes, including the use of inert cushion gases. Because it is a module of TOUGH2, EOS7C includes all of the multiphase flow capabilities of TOUGH2, including the ability to model water drives and gas-liquid displacements that may be present in gas reservoirs.

#### Application To Rio Vista Gas Field

In this section, we investigate by numerical simulation the process of CSEGR at the Rio Vista Gas Field. Rio Vista is the largest gas field in California and has been under production since 1936.<sup>15</sup> It is located approximately 75 km northeast of San Francisco in the Sacramento Basin and has an elongated dome-shaped structure extending over a 12 by 15 km area (see Figure 3). The reservoir rocks are Upper Cretaceous to Eocene and consist of alternating layers of sands and shales deposited in deltaic and marine environments. Normal faulting occurred contemporaneously with sedimentation, creating a set of sub-parallel faults trending NW through the field. The most important of these is the Midland Fault (Figures 3 and 4). In some gas-bearing strata, displacement along the faults has created structural traps. In others, particularly the thicker gas bearing sands, the smaller faults do not play as important a role in defining reservoir structure.

Since 1936 the Rio Vista Gas Field has produced from 365 wells over  $9.3 \times 10^{10}$  m<sup>3</sup> of natural gas (at standard conditions of 1 bar, 15.5 °C [14.7 psi, 60 °F]). Assuming a CH<sub>4</sub> density of 0.678 kg m<sup>-3</sup> (1 bar, 15.5 °C), this volume corresponds to a mass of  $6.3 \times 10^{10}$  kg. Production peaked in 1951 with annual production of  $4.4 \times 10^9$  m<sup>3</sup> and, as shown in Figure 5, has declined steadily since then.<sup>16</sup> Production decline is caused by decreasing

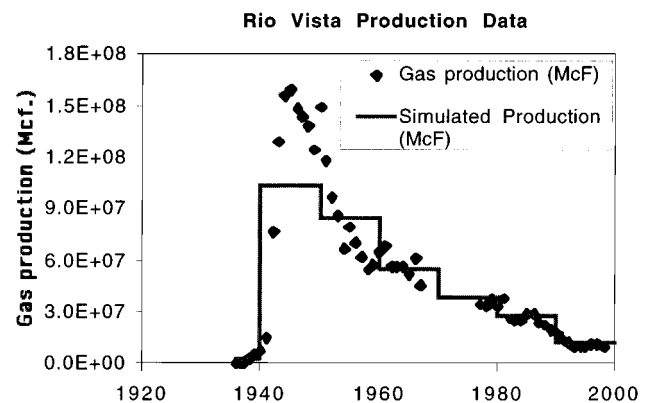


Figure 5. Production history of methane from the Rio Vista Gas Field. Production from model system is 1/16 of the 10-year-averages shown. (n.b., 1 Mcf = 10<sup>3</sup> cf)

reservoir pressures and increased water production, particularly on the western boundary of the field.

The Domengine formation shown in Figure 4 has been the most productive pool in the Rio Vista Gas Field. It occurs at an average depth of 1150 to 1310 m with an average net thickness of 15 to 100 m. The initial reservoir pressure and temperature were approximately 120 bar and 65 °C. Other generalized reservoir properties are provided in Table 2. As shown in Figure 4, the Domengine is laterally continuous across the Rio Vista Gas Field with vertical confinement provided by the Nortonville and Capay Shales. Its western boundary is controlled by the presence of the water table at a depth of 1325 m. For the purpose of this study we focused on CO<sub>2</sub> sequestration and enhanced gas recovery in the Domengine formation to the west of the Midland Fault (see Figure 4).

The source of CO<sub>2</sub> considered in this study is the 680 MW gas-fired power plant located in Antioch, California (20 km from Rio Vista). This plant produces  $2.2 \times 10^9$  m<sup>3</sup> (1 bar, 15.5 °C) or  $4.15 \times 10^9$  kg (4.15 MT) of CO<sub>2</sub> annually. Assuming a CH<sub>4</sub> density of 78.1 kg m<sup>-3</sup> (122 bar, 65 °C), the volume formerly occupied by CH<sub>4</sub> produced since 1936 is  $8.1 \times 10^8$  m<sup>3</sup> ( $6.3 \times 10^{10}$  kg/78.1 kg m<sup>-3</sup> =  $8.1 \times 10^8$  m<sup>3</sup>). At these same reservoir conditions (122 bar, 65 °C), the density of CO<sub>2</sub> is 409.6 kg m<sup>-3</sup>, which suggests that approximately 80 years of sequestration capacity are available at Rio Vista ( $8.1 \times 10^8$  m<sup>3</sup> × 409.6 kg m<sup>-3</sup> /  $4.15 \times 10^9$  kg CO<sub>2</sub> year<sup>-1</sup> = 79.9 years).

The simplified 2-D model system based on the Rio Vista Gas Field is shown in Figure 6. The model system is a 1 km wide cross-section with vertical dimensions

(12) Irvine, T. F., Jr.; Liley, P. E. *Steam and gas tables with computer equations*; Academic Press: Orlando, FL, 1984; 185 pp.

(13) Cramer, S. D. *The solubility of methane, carbon dioxide and oxygen in brines from 0° to 300 °C*; U. S. Bureau of Mines: Report No. 8706, 1982; 16 pp.

(14) Pritchett, J. W.; Rice, M. H.; Riney, T. D. *Equation-of-state for water-carbon-dioxide mixtures: implications for Baca reservoir*; Report DOE/ET/27163-8, UC-66-a, 1981; 53 pp.

(15) Burroughs, E. *Rio Vista Gas Field. Summary of California oil fields*; State of California, Department of Conservation, Division of Oil and Gas: 1967; 53, No. 2-Part 2, pp 25–33.

(16) Cummings, M. F. *Northern California oil and gas field production. Annual production and well Data, 1977–1998*; State of California, Division of Oil, Gas and Geothermal Resources: 1999.

(17) van Genuchten, M. Th. *Soil Sci. Soc.* **1980**, *44*, 892–898.

**Table 2. Relevant Properties of Rio Vista Model Gas Reservoir**

property	value	units
porosity	0.35	—
Y, Z-direction permeability	$1.0 \times 10^{-12}$ , $1.0 \times 10^{-14}$	$\text{m}^2$ , $\text{m}^2$
capillary pressure	van Genuchten model <sup>17</sup>	—
$m$ , $S_{lr}$ , $1/\alpha$ , $P_{\text{capmax}}$ , $S_{ls}$	0.2, 0.27, $8.4 \times 10^{-4}$ , $-10^5$ , 1	—, —, $\text{Pa}^{-1}$ , $\text{Pa}$ , —
relative permeability	van Genuchten model <sup>17</sup>	—
liquid	—	—
gas	Corey model ( $S_{gr} = 0.01$ )	—
molecular diffusivity in gas, liquid	$1.0 \times 10^{-5}$ , $1.0 \times 10^{-10}$	$\text{m}^2 \text{s}^{-1}$ , $\text{m}^2 \text{s}^{-1}$
temperature	65	$^{\circ}\text{C}$
initial pressure at water table	126	bars

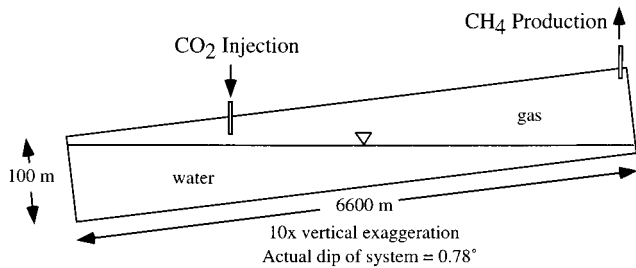


**Figure 6.** 2-D vertical section used in CSEGR simulations.

100 m and horizontal extent 6600 m of the western flank of the dome, corresponding to 1/16 of the actual length of the reservoir. The model system was discretized into 660 gridblocks ( $33 \times 20$ ) of sizes  $200 \text{ m} \times 5 \text{ m}$  in Y- and Z-directions, respectively. The model reservoir has a roof sloping at 0.78 degrees to the west. The bottom of the gas reservoir is a horizontal water table. Note that in all simulations presented here, water drive is turned off by closing all the lower boundaries of the system. Properties of the formation are simplified for this study as shown in Table 2.

The initial condition consists of the water table at  $Z = 0$  on the left-hand side of the domain at a pressure of 126 bar, with  $\text{CH}_4$  gas and residual water ( $S_{lr} = 0.27$ ) in the pore space above. All simulations were done at isothermal conditions of  $65 \text{ }^{\circ}\text{C}$ . From this initial condition, we simulated the withdrawal of  $\text{CH}_4$  at 1/16 the historical rate as shown in Figure 5 for the period 1936–1998.

Following the historical production, we simulated  $\text{CO}_2$  injection at a point 15 m below the top of the reservoir at approximately  $Y = 2000 \text{ m}$ , and  $\text{CH}_4$  withdrawal from

the upper right-hand side of the domain ( $Y = 6600 \text{ m}$ ). In all cases,  $\text{CO}_2$  is injected into the reservoir at a rate corresponding to 1/16 the actual production of  $\text{CO}_2$  from the 680 MW Antioch gas-fired power plant. An example simulation result from Scenario I, where  $\text{CO}_2$  is injected into the reservoir for 10 years with no  $\text{CH}_4$  production, is presented in Figure 7. Contours of mass fraction of  $\text{CO}_2$  in the gas and vectors of gas velocity clearly show the  $\text{CO}_2$  migration and depression of the water table below the injection point in response to gas injection. As gas is injected, reservoir pressure increases with limited mixing of the gases by advection and diffusion. In Figure 8, we show simulation results for the second part of Scenario I where  $\text{CO}_2$  injection is stopped and  $\text{CH}_4$  production occurs for 10 years.

Summaries of the simulated pressure evolutions and mass production rates are shown in Figures 9 and 10, respectively. The two different scenarios we considered start in 1999 (see Table 3). In Scenario I,  $\text{CO}_2$  is injected into the reservoir for 10 years as shown in Figure 7. This injection serves to repressurize the reservoir. In the subsequent part of Scenario I,  $\text{CH}_4$  is produced for 10 years from the repressurized reservoir at a rate corresponding to the 1950–1960 average rate as shown in Figure 8. In Scenario II,  $\text{CO}_2$  injection is simultaneous with  $\text{CH}_4$  production, where  $\text{CH}_4$  is produced at constant pressure. Note in Figure 9 that in Scenario I, 99% pure  $\text{CH}_4$  can be produced for approximately five years following  $\text{CO}_2$  injection, and that this  $\text{CH}_4$  production is at a very high rate. In Scenario II, 99% pure  $\text{CH}_4$  can be produced for approximately five years during  $\text{CO}_2$  injection, although the rate is smaller than in Scenario I (see Figure 10). The duration of the enhanced recovery

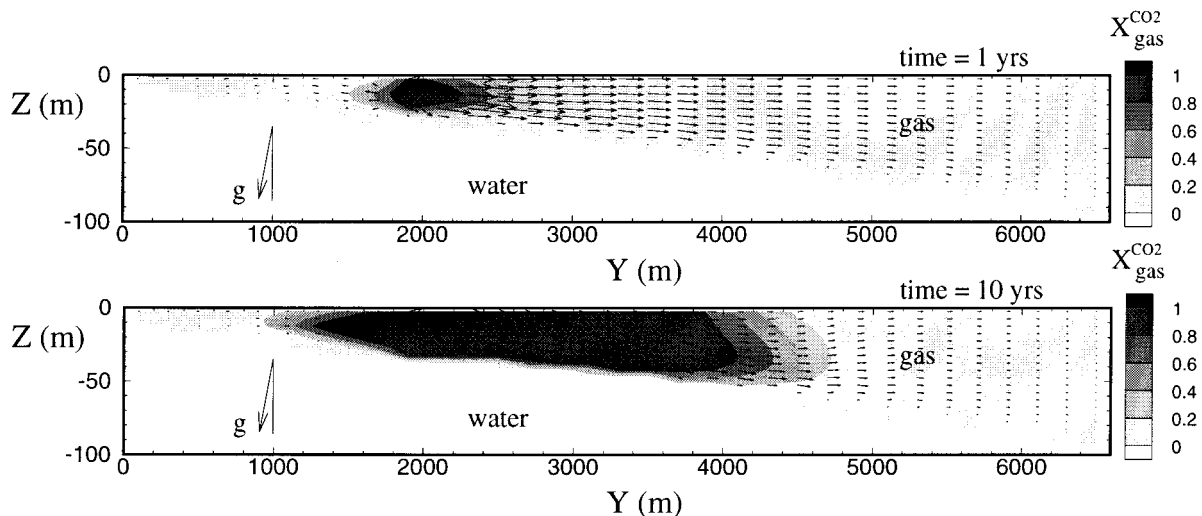


**Figure 7.** Mass fraction of  $\text{CO}_2$  in the gas phase and gas velocity at  $t = 1$  year and 10 years with no  $\text{CH}_4$  production.

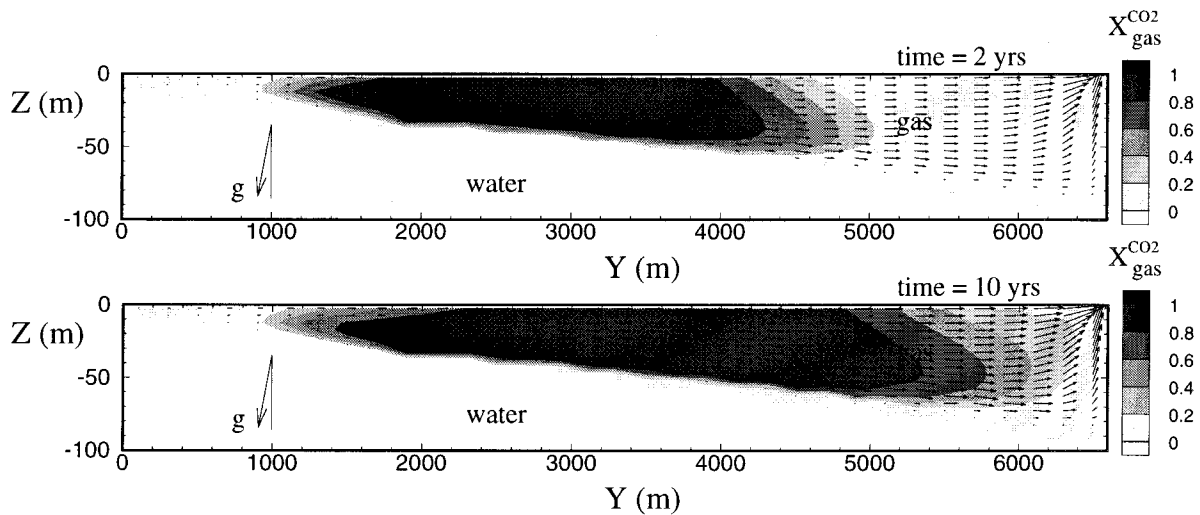


**Figure 8.** Mass fraction CO<sub>2</sub> in the gas phase and gas velocity after 2 and 10 years of CH<sub>4</sub> production following 10 years of CO<sub>2</sub> injection.

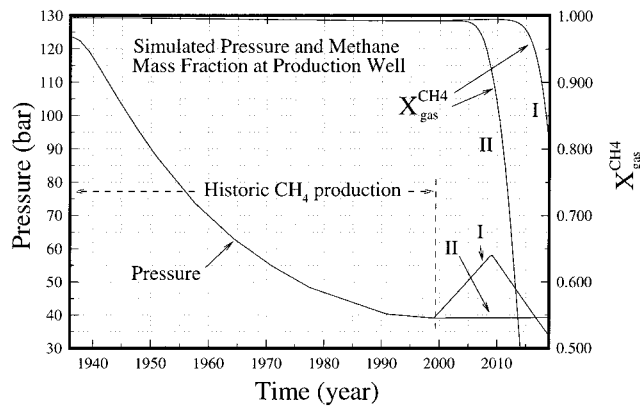


**Figure 9.** Pressure and CH<sub>4</sub> mass fraction evolution for Scenarios I and II.

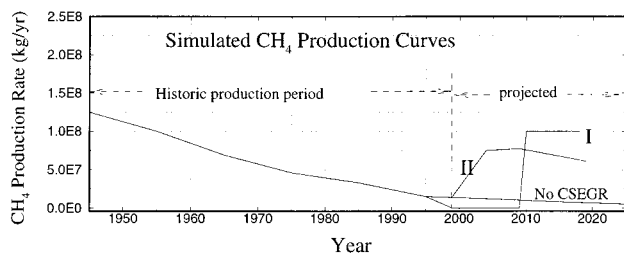


**Figure 10.** Simulated mass production rates of CH<sub>4</sub> for Scenarios I, II, and projected if no CSEGR.

period depends on the tolerance of the operator for CO<sub>2</sub>, the concentrations of which increase with time in the produced gas. The total additional masses of CH<sub>4</sub> produced by CSEGR for Scenarios I and II are 9.8 × 10<sup>8</sup> kg (5.1 × 10<sup>7</sup> Mcf) and 1.4 × 10<sup>9</sup> kg (7.3 × 10<sup>7</sup> Mcf), respectively, as compared to a projected 1.8 × 10<sup>8</sup> kg (9.4 × 10<sup>6</sup> Mcf) without CSEGR. Note that these quantities are for the 2-D model system which is 1/16 of the whole gas field.

We present in Figure 11 a scenario to examine the process of density stratification within the reservoir for the case of no CH<sub>4</sub> production. In this scenario, CO<sub>2</sub> is injected for 10 years and then allowed to migrate as driven by density and pressure gradients. As seen in Figure 11, CO<sub>2</sub> moves downward due to its greater density relative to CH<sub>4</sub>. Density stratification tends to inhibit mixing and favors CSEGR where production wells can be screened in upper regions of the reservoir.

Because of the large gridblock sizes and relatively large gas-phase velocities, the simulations presented here include significant numerical dispersion which tends to overpredict gas-phase mixing. Meanwhile the simulations have neglected hydrodynamic dispersion which would also increase gas-phase mixing. However, the numerical dispersion mixing length is of the same order (approximately 1 km) as the hydrodynamic dispersion mixing length assuming a longitudinal dispersivity of 100 m and 20 years of CSEGR. Therefore in this case, the effects of numerical dispersion in the simulations approximately mimic hydrodynamic dispersion. Hydrodynamic dispersion can be an important mixing mechanism, but for slow gas velocities and over large length scales, reservoir repressurization by CO<sub>2</sub> injection and production of high quality CH<sub>4</sub> is possible.

### Conclusions

Properties of natural gas reservoirs and of CO<sub>2</sub> and CH<sub>4</sub> are favorable for repressurization without extensive mixing over time scales of practical interest. Simulations of the process of CO<sub>2</sub> injection into a depleted natural gas reservoir carried out with TOUGH2/EOS7C confirm the plausibility of CSEGR as a way to sequester carbon while enhancing CH<sub>4</sub> recovery. Simulations that use realistic estimates of CO<sub>2</sub> produced from the Antioch

**Table 3. CSEGR Scenarios for Rio Vista Case Study**

period	inject	produce	rate	cumulative mass
1936–1998	–	CH <sub>4</sub>	variable (1/16 historical CH <sub>4</sub> production)	–3.5 × 10 <sup>9</sup> kg CH <sub>4</sub>
Scenario I.	CO <sub>2</sub>	–	8.2 kg/s (1/16 Antioch CO <sub>2</sub> production)	2.6 × 10 <sup>9</sup> kg CO <sub>2</sub>
1999–2009	–	CH <sub>4</sub>	3.2 kg/s (1950–1960 average rate)	–9.8 × 10 <sup>8</sup> kg CH <sub>4</sub>
2010–2019	–	CH <sub>4</sub>	CO <sub>2</sub> : 8.2 kg/s	5.1 × 10 <sup>9</sup> kg CO <sub>2</sub>
Scenario II.	CO <sub>2</sub>	CH <sub>4</sub>	CH <sub>4</sub> : variable (constant pressure of 39 bar)	–1.4 × 10 <sup>9</sup> kg CH <sub>4</sub>

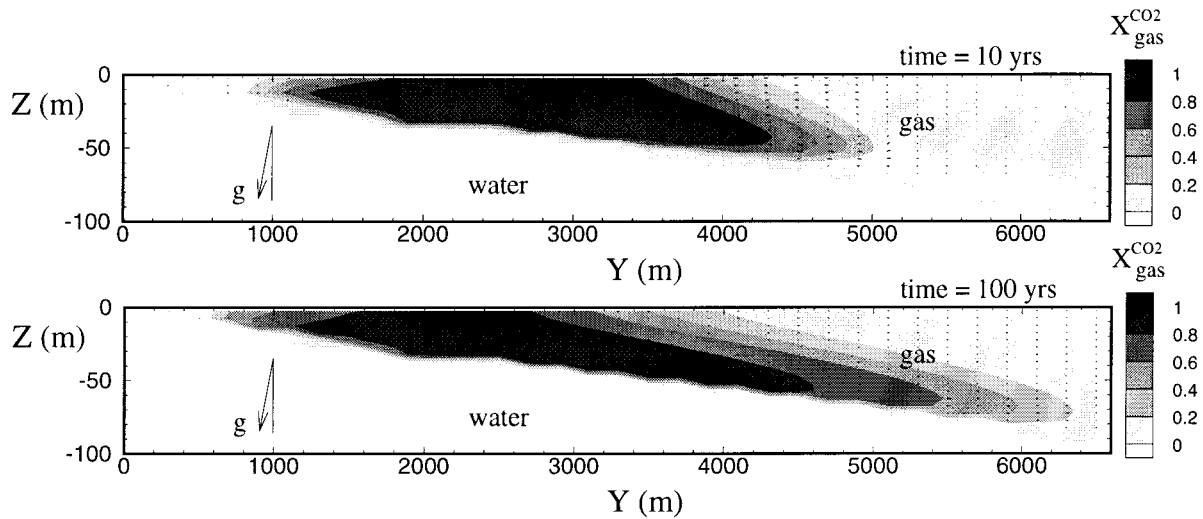


**Figure 11.** Mass fraction CO<sub>2</sub> in the gas phase and gas velocity at  $t = 10$  years and 100 years for the case of gravity-driven density stratification following 10 years of CO<sub>2</sub> injection.

gas-fired power plant show that CSEGR allows more than five times the mass of CH<sub>4</sub> to be recovered relative to that which would be produced without CSEGR. The Rio Vista Gas Field is a potential site for CSEGR.

**Acknowledgment.** The authors thank Drs. P. Witherspoon and L. Myer of Lawrence Berkeley National Laboratory for fruitful discussions regarding the feasibility of carbon sequestration and enhanced gas recovery. We also acknowledge the help of M. F. Cummings of the California Division of Oil and Gas in obtaining detailed production data for the Rio Vista Gas Field.

Thanks are also due to Victoria Porto who helped gather the early data needed for this project. The comments of two anonymous reviewers led to improvements in the presentation. This work was supported by the Assistant Secretary for Fossil Energy, Office of Coal and Power Systems through the National Energy Technology Laboratory, and by Laboratory Directed Research and Development Funds at Lawrence Berkeley National Laboratory under Department of Energy Contract No. DE-AC03-76SF00098.

EF000247H